

Optimizing performance parameters of stationary wire free power transfer circuit

Raja Vidya¹, Belur K. Keshavan²

¹Department of Electrical and Electronics Engineering, RV College of Engineering, Bangalore, India

²Department of Electrical and Electronics Engineering, PES University, Bangalore, India

Article Info

Article history:

Received Sep 16, 2022

Revised Feb 25, 2023

Accepted Mar 6, 2023

Keywords:

Electric vehicles

Maximum efficiency

Optimization

Performance parameters

Wire free power transfer

ABSTRACT

The power efficiency of the wire free power transmission (WPT) system is tested in this article under various transmission distance circumstances, and the findings are utilized to investigate the best way to regulate the parameters for charging electric vehicles (EVs). The system's power transfer efficiency is improved over using a fixed resonant frequency by altering it in response to changes in the coupling coefficient. In relation to resonance frequency, a trade-off between output power magnitude and power efficiency is also revealed. Through numerical simulation with Ansys, the trade-off resonant frequencies at various transmission lengths are determined by the analysis. Here, the transmitter and receiver employ circular coils with a circular cross-sectional area and a straightforward but effective series-series (SS) compensation architecture is used for comprehensive analysis.

This is an open access article under the [CC BY-SA](#) license.



Corresponding Author:

Raja Vidya

Department of Electrical and Electronics Engineering, RV College of Engineering

Bangalore, India

Email: rajavidya@rvce.edu.in

1. INTRODUCTION

The uses of wire-free power transmission (WPT) technology [1]–[3] in electric vehicles (EVs), medical implants, consumer electronics, mining, and underwater charging have made significant strides. This technique is used in situations where it would be impractical, costly, dangerous, or even impossible to deliver electricity via standard wired wires. The use of wire free power transmission in electric vehicles (EVs) is seen to be a viable way to combat the problem known as “range anxiety,” which is the most popular word used to describe it. EVs may charge more quickly with both fixed and dynamic wire free power transfer methods, with the latter even enabling seamless operation without ever needing a stoppage to charge. The schematic illustration of the stationary WPT system is shown in Figure 1. One of the reasons to embrace EVs is the opportunity to significantly lower the capacity of energy storage while increasing the driving range. As a result, all interested academics are focusing their attention on the study of EV wireless charging solutions.

The power is transferred via the mutual induction principle using WPT technology. Power is transmitted from one electrically separated but magnetically coupled circuit to another using the electrical transformer principle. Power is transferred in a transformer between coils that are closely linked and wrapped on a single common core that is shared by both the primary and secondary windings. With the WPT system, primary winding serves as the transmitter and secondary winding serves as the receiver, with no shared core in between. Both the transmitter and receiver coils are separated by an air medium. Therefore, planar coils are employed. These coils might have cross sections that are square, rectangular, or circular and come in circular, square, or double D (DD) geometrical shapes. The WPT system's effectiveness is greatly influenced by the coil's design, geometry, type, internal and exterior diameter, width, area of cross section, number of

turns, number of strands and spacing between turns. Authors Mentions a thorough coil design for a 3.7 kW WPT charger with several coil topologies [4]. In WPT systems, compensations are typically needed to increase efficiency while lowering the inverter's VA rating. Series-series (SS) compensation [5], parallel-parallel (PP) [6], SP and PS compensation [7], [8] and LCC compensation [9], [10] are a few examples of the typical compensations. The structure of series-series capacitor compensation along with the rest of the WPT system is depicted in Figure 2.

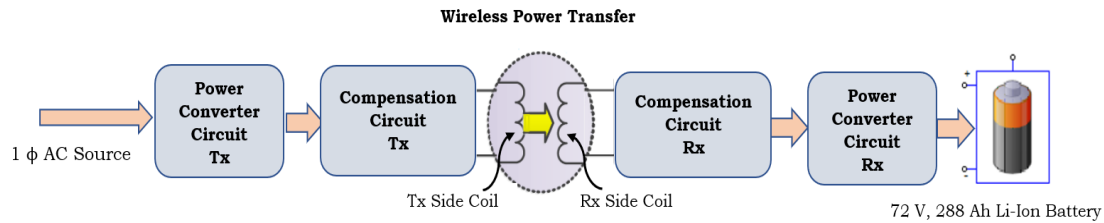


Figure 1. Block diagram of stationary WPT system

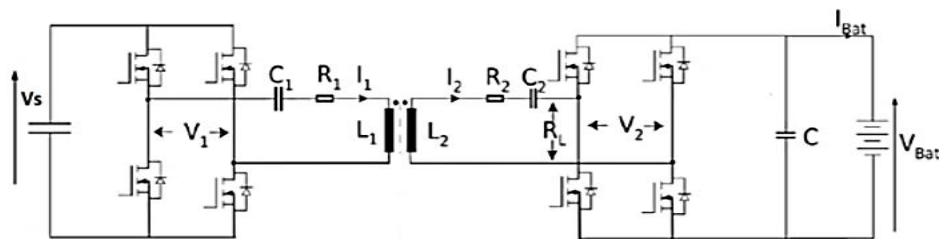


Figure 2. The wire free system model for SS topology

The voltage from the rectifier's output is shown as V_s in Figure 2, and V_1 is the voltage across the high-frequency inverter that powers the transmitter coil together with the series compensation circuit C_1 in the figure. In a similar manner, C_2 is offered in series with the receiver coil. When the battery in a car is being charged using a constant current and constant voltage profile, V_2 is the voltage across the rectifier that is being employed. I_{Bat} is an illustration of the battery current needed for charging, while V_{Bat} shows the voltage across the battery.

The series-series compensation topology has been demonstrated by Chopra *et al.*, [11] to be one of the better alternatives since resonant circuits may be built regardless of coupling and load. Prasanth [12] describes capacitance at the main relies on load in the parallel-parallel compensation topology, and its implementation is simpler than that of series-series topologies. The benefits of series-parallel resonant coupling over SS based on a longer power transfer distance and over parallel topology based on a higher power transfer efficiency have been explored by Chen *et al.* [13] and Villa *et al.* [14]. Villa *et al.* [14] have studied the tolerance for transmitter and receiver misalignment with experimental evidence.

According to the findings from [15], [16] literatures, highly flexible compensation topologies, integration methods, and relative control strategies for high misalignment-tolerant WPT system were discussed. Rehman *et al.* demonstrated, power is conveyed using a magnetic resonance technology with a maximum efficacy of 96% at a distance of 60 cm between the two coils. The technique's effectiveness was empirically and mathematically validated by Rehman *et al.* [17]. The authors have demonstrated that misalignment may be completely removed by using a network analyzer and an automated 3-axis platform for the control of motion of the coil. According to experimental findings, the target 90% power transfer efficiency was attained at a misalignment ratio of 0.5 and a ratio of air-gap ranges between 0-0.25 [18], [19]. WPT misalignment problems can be overcome by utilizing a ferrite core since ferrites are more effective and tolerant of misalignment. The LCL-Series topology from the Hybrid topologies is a variation of compensation architecture that allows an uninterrupted flow of current as well as output voltage in the transmitter, independent of the EV's misalignment [20]. Klaus *et al.* [21] asserted that there appeared to be a considerable electromagnetic field leakage between the transmitter and the reception coil as a result of the wide air gaps. As a result of the threat this electromagnetic field leakage poses to people, it is crucial to reduce the magnetic leakage between the two coils. To lessen magnetic leakage between the two coils, a dual-sided LCC compensation structure and associated tuning techniques have been explored in [22].

Various aspects of WPT systems are studied at different research centers of late. In the paper described by Li *et al.* [23], major emphasis has been laid on study of resonance circuits and non-resonance circuits. Though the authors have not taken into account how optimum resonance frequency is used for obtaining high efficiency, they were intended to provide electricity to moving vehicles, through a wirefree power transmission system [24]. However, none of these situations assess the performance metrics' ideal circumstances. The impacts of load and air gap fluctuations are investigated for various compensation designs using an inductive power transfer (IPT) system that is developed for a rotating transformer [10]. However, it is not taken into account how much the operating frequency variation would affect system efficiency. For the design of an inductively coupled power transfer circuit with various compensation structures for a public transportation system, an IPT optimization technique is used [25]. It should be noted that the system's efficiency is not assessed for various operating scenarios with varying coupling coefficients and frequency. Under various loading scenarios, a base frequency is discovered for the best performance of electrically isolated transformers [26]. System limitations are not controlled, nevertheless, in order to achieve high efficiency for various case studies, it is essential to conduct a thorough analysis of the factors influencing wire free power transmission efficiency while developing the hardware for practical use.

Several optimization strategies with circuit modelling are discussed in several recent research [27], [28] to increase power transfer efficiency. To maximize efficiency in real-world settings, Heidarian and Burgess [29] suggested simple approximation techniques for Tx sources and Rx loads. The proposed method produced some inconsistencies in terms of maximum efficiency when compared to the genetic algorithm (GA) and the maximum Rayleigh quotient method, but it was simple to use in practice for a grotesquely rough estimation of the system. In order to determine the best placements and the ideal length of dynamic wireless charging lanes at each location, Lee and Lee [30] recognized unforeseen problems in dynamic wireless charging and to maximize the system's overall energy transfer capability, they used traffic simulations and non-linear optimization techniques. Meligy *et al.* [31] used the finite element method to compute and model the mutual inductance between the transmitting and receiving coil. For a series-series resonant circuit, the impact of changing the supply frequency, load, axial distance, and lateral misalignment on power efficiency is simulated. Authors increased power efficiency with changing axial lengths and lateral misalignment by using an impedance matching network (IMN). Abdelhamid *et al.* [32], evaluated a number of cutting-edge strategies that have been developed over the past few years, including optimization techniques to increase power transfer efficiency and a study focusing on ways to minimize battery size. A review of electric vehicle (EV) technology, charging systems, and optimization approaches has been published by Patil and Gadgune [33]. The most popular optimization methods for size and positioning EV charging stations have been discussed by the authors. The spatial parameters of the coil group and the parameters of the compensation circuit are chosen by Prakash *et al.* [34], as input variables, and the deep learning network is then constructed as the framework for estimating uncertainty. To acquire the pertinent statistical characteristic parameters of WPT efficiency, this is necessary. By contrasting the calculation results of the standard Montecarlo algorithm, the authors were able to demonstrate that the uncertainty quantification based on deep learning algorithm has almost the same solution accuracy and superior computing efficiency. The standard aquila optimization (AO) algorithm was improved by the author using tent chaotic mapping and an adaptive inertia weight strategy. The improved multi objective AO algorithm was then applied to optimize the structure of the WPT system.

Two crucial metrics of a WPT system, power transfer efficiency (PTE) and power delivered to the load (PDL), were discussed by Wang *et al.* [35]. They have noted that the important indications are reliant on a number of WPT system design factors, including the operating frequency, the geometrical characteristics of the coils, and the distance between the coils used for transmission and reception (TX and RX). In order to optimize the major indicators in the WPT system, metaheuristic algorithms were applied. The impact of lowering the losses (resistances) of intermediate circuits on the active power values communicated to the load and on the power transfer efficiency values has been examined by Ouacha *et al.* [36]. Iordache *et al.* [37] compared a wireless power transfer system (WPTS) with six magnetic couplings to three magnetic couplings. The optimization algorithms presented in this paper were suitable for calculating the optimal parameters of the WPTS equivalent circuit and through the proposed technique, the minimum and maximum performance values were obtained.

Analytical discussion of the resonance frequency and coupling coefficient of an inductively coupled resonant circuit is presented in this paper. The air gap separating the two coils, the system structure (with or without ferrites and aluminium), the self and mutual inductances, and all of these variables are crucial to the analytical calculations. Coil-to-coil efficiency and coupling factor (k) are utilised as performance measurements, and a detailed analysis is done to find out how these metrics affect and change the performance of the system. Increased system performance is achieved through frequency and load optimisation.

2. THE PROPOSED WPT SYSTEM MODELLING

According to Figure 1, the wirefree power transfer circuit utilizes resonance technology and is defined by inductive principles. A high frequency voltage linked to the transmitter coil in series with it powers the circuit, along with the resonant capacitor C_1 and the coil series resistance R_1 . Figure 3 illustrates two circular bare coils (without ferrite core) with self-inductances L_1 and L_2 that are having a mutual inductance M .

The geometric parameters for both the circular coils are mentioned in Table 1. On the receiver side, symmetry is maintained with Series resistance R_2 and resonant capacitor C_2 . The converter circuit including the battery is acting as an equivalent load resistance R_L .

This paper focuses on optimizing the operations of performance parameters both under normal alignment and misalignment. The concept is explained based on the topology of basic circuit theory. Figure 2 is modified as shown below into Figure 4, illustrating the simplified WPT model with SS topology. Were i) R_1 : Resistance of coil L_1 ; ii) R_2 : Resistance of coil L_2 ; iii) C_1 : Primary resonance capacitance; iv) C_2 : Secondary resonance capacitance; v) V_{in} : Input voltage (high frequency); vi) L_1 : Primary coil self-inductance; vii) L_2 : Secondary coil self-inductance; and viii) R_L : Load resistance.

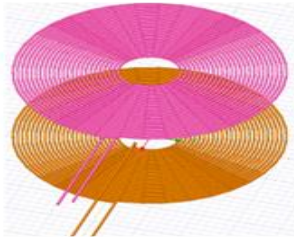


Figure 3. Circular coils (bare coils)

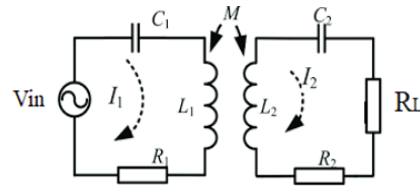


Figure 4. Simplified WPT model for SS topology

Table 1. Geometric parameters for circular coils

| Parameters | Dimensions | Parameters | Dimensions |
|------------------------|------------|----------------------------------|------------|
| Internal Diameter (di) | 129 mm | No of Transmitter Turns(N_1) | 24 |
| External Diameter (de) | 597 mm | No of Receiver Turns(N_2) | 24 |
| Turns Spacing (S) | 6 mm | Airgap Distance | 180 mm |
| Turn Width(W) | 4 mm | | |

The circuit is further realized as coupled coils with mutual inductance M , and modelled with equivalent circuit, as shown in Figure 5. Let's consider two similar coils having the same number of turns, area of cross section, internal diameter and external diameter as mentioned in Table 1.

Hence, $L_1=L_2=L$ & Mutual Inductance $M=K\sqrt{L_1L_2}$.

$$\therefore M = KL.$$

From the equivalent WPT circuit as shown in Figure 5, let $j\omega Mi_2$ and $j\omega Mi_1$ are dependent voltage source in primary and secondary side respectively. With reference to Figure 5, impedance at the primary side is given by (1).

$$Z_1 = R_1 + \frac{1}{j\omega C_1} + j\omega L_1 \quad (1)$$

Impedance at the secondary side is given by (2).

$$Z_2 = R_2 + \frac{1}{j\omega C_2} + j\omega L_2 + R_L \quad (2)$$

Now the expression for current at the secondary side is given by (3),

$$i_2 = \frac{-j\omega M i_1}{Z_2} \quad (3)$$

and the dependent voltage source at the primary is (4).

$$j\omega M i_2 = j\omega M * \frac{-j\omega M i_1}{Z_2} \quad (4)$$

So,

$$j\omega M i_2 = \frac{\omega^2 M^2}{Z_2} * i_1 \quad (5)$$

and

$$j\omega M i_2 = Z_{eq} i_1 \quad (6)$$

where Z_{eq} is the equivalent impedance of secondary referred to primary.

$$Z_{eq} = \frac{\omega^2 M^2}{Z_2} \quad (7)$$

The dependent voltage source at the primary can be replaced by equivalent impedance Z_{eq} .

$$Z_{eq} = \frac{\omega^2 M^2}{Z_2}$$

$$Z_{eq} = \frac{(\omega K \sqrt{L_1 L_2})^2}{Z_2} \quad (8)$$

$$Z_{eq} = \frac{\omega^2 K^2 L^2}{Z_2} (\because L_1 = L_2 = L) \quad (9)$$

Considering $\omega = \frac{1}{\sqrt{L_1 C_1}} = \frac{1}{\sqrt{L_2 C_2}}$ as the primary circuit and secondary circuit resonates at equal frequency.

That is $X_{L1} = \frac{1}{X_{C1}}$ and $X_{L2} = \frac{1}{X_{C2}}$.

\therefore The total impedance at the secondary will be,

$$R_L^1 = Z_2 = R_L + R_2 \quad (10)$$

and now, output power across the load R_L is given by (11),

$$P_0 = i_2^2 R_L \quad (11)$$

and the new value of equivalent impedance referred to primary would be,

$$Z_{eq} = \frac{\omega^2 M^2}{R_L + R_2} = \frac{\omega^2 M^2}{R_L^1}$$

where $R_L^1 = Z_2 = R_L + R_2$ from (10) and hence the new value of i_2 is,

$$i_2 = \frac{-j\omega M i_1}{R_L^1}$$

and

$$i_2^2 = \frac{\omega^2 M^2}{(R_L^1)^2} * i_1^2 \quad (12)$$

\therefore Power delivered at the output across the load is given by,

$$P_0 = \frac{\omega^2 M^2}{(R_L^1)^2} * i_1^2 R_L$$

which can be rewritten as (13).

$$P_0 = i_1^2 * \frac{\omega^2 M^2}{R_L + R_2} * \frac{R_L}{R_L + R_2} \quad (13)$$

But

$$\frac{\omega^2 M^2}{R_L + R_2} = \frac{\omega^2 K^2 L^2}{R_L^1}$$

So, from (13) power at the output depends on the load resistance, frequency of the transferred power and the mutual inductance between the coupled coils. In turn power transferred at the output depends on Coupling coefficient k . To find an expression for efficiency, let's find the value of the impedance Z_1 and Z_2 .

$$Z_2 = R_2 + R_L + \frac{1}{j\omega C_2} + j\omega L_2 \quad (14)$$

We know that $Z_{eq} = \frac{(\omega M)^2}{Z_2}$ [secondary impedance referred to primary]

$$\therefore Z_1 = R_1 + \frac{1}{j\omega C_1} + j\omega L_1 + Z_{eq} \quad (15)$$

at resonance, the reactive components seen from primary and secondary is zero.

$$i.e. \frac{1}{j\omega C_2} = j\omega L_2 \quad [\because X_{L2} = X_{C2}] \quad \& \quad \frac{1}{j\omega C_1} = j\omega L_1$$

$$\therefore Z_2 = R_2 + R_L = R_L^1 \quad (16)$$

$$Z_{eq} = \frac{(\omega M)^2}{R_L + R_2} = \frac{(\omega M)^2}{R_L^1}$$

$$Z_1 = R_1 + Z_{eq} = R_1 + \frac{(\omega M)^2}{R_L + R_2} \quad (17)$$

From the fundamentals, % Efficiency = % η = ((output power)/ (Input Power)) *100. That is $\eta = \frac{P_{out}}{P_{in}}$ where, Input power applied from the output of High frequency inverter,

$$P_{in} = i_1^2 Z_1 = i_1^2 [R_1 + \frac{(\omega M)^2}{R_L + R_2}] \quad (18)$$

and output power across the load is given by (19) and (20),

$$P_{out} = i_2^2 Z_2 = i_2^2 (R_2 + R_L) = \frac{(\omega M)^2}{(R_L + R_2)^2} * i_1^2 (R_2 + R_L) \quad (19)$$

$$[\because i_2^2 = \frac{(\omega M)^2}{(R_L + R_2)^2} * i_1^2]$$

$$\therefore P_{out} = [\frac{(\omega M)^2}{R_L + R_2}] * i_1^2 \quad (20)$$

from (18) and (20),

$$\therefore \eta = \frac{P_{out}}{P_{in}} = \frac{\frac{(\omega M)^2}{R_L + R_2} * i_1^2}{R_1 + [\frac{(\omega M)^2}{R_L + R_2}] * i_1^2}$$

$$\therefore \eta = \frac{(\omega M)^2 R_L}{R_1 (R_L + R_2)^2 + (\omega M)^2 (R_L + R_2)} \quad (21)$$

From efficiency in (21), it is noticeably clear that, coil to coil efficiency depends on resonance frequency, coupling coefficient and the load resistance. The derivation is done by considering all the vital parameters of the WPT circuit. Now, Figure 6 depicts the block diagram showcasing coil to coil and overall efficiency of the WPT system. This paper considered coil to coil efficiency for further analysis.

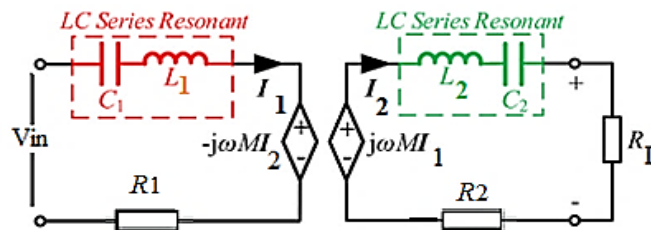


Figure 5. Equivalent WPT circuit

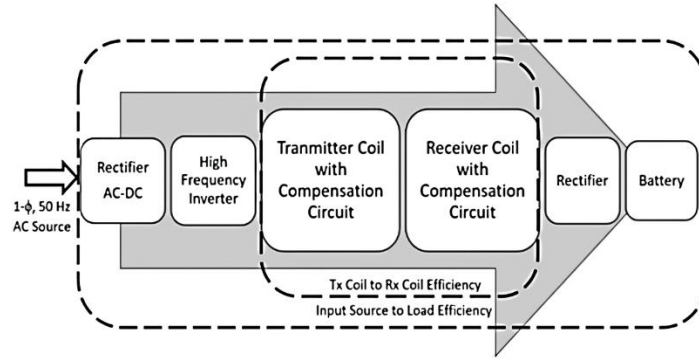


Figure 6. Efficiency consideration of stationary WPT System

3. RESEARCH METHOD - OPTIMIZATION TO ACHIEVE MAXIMUM EFFICIENCY

As previously mentioned, the electromagnetic structure of the coil and its components, including the load, operating frequency, and coupling coefficient, have a significant impact on the performance of WPT systems. The settings need to be tweaked for the best system performance. A mutual coupling optimization technique is used to optimize the performance parameters in WPT system. Let's consider load optimization:

$$\frac{d\eta}{dR_L} = \frac{d}{dR_L} \left\{ \frac{(\omega M)^2 R_L}{R_1 (R_L + R_2)^2 + (\omega M)^2 (R_L + R_2)} \right\} = 0$$

$$\therefore R_{L(Opt)} = R_2 \sqrt{1 + \frac{(\omega M)^2}{R_1 R_2}} \quad (22)$$

and similarly, if the operating frequency is optimized.

$$\frac{d\eta}{df_0} = 0$$

Then,

$$f_{Optimum} = \frac{1}{2\pi \sqrt{L_2 C_2 - \frac{[C_2 (R_L + R_2)]^2}{2}}} \quad (23)$$

in comparison to load resistance R_L and $R_1, R_2, R_L \gg R_1, R_L \gg R_2, (\omega M)^2 \gg R_1, (\omega M)^2 \gg R_2$, and $R_1 \approx R_2$, the maximum efficiency expression would be,

$$\therefore \eta_{Opt} = \frac{k^2 R_L L_1}{k^2 L_1 (R_L + R_2) + R_1 C_2 (R_L + R_2)^2} \quad (24)$$

Coupling coefficient k , which represents the intensity of electromagnetic coupling, is dependent on the parameters of primary and secondary windings, air gap and the effect of ferrite core. Most of these parameters are stationary except the distance between the coils, which is in reciprocal to coupling coefficient and efficiency, and can be changed. Hence optimization of few parameters is required to get maximum efficiency. Let's apply these concepts to circular coils. Here two cases are discussed: i) Circular coils without ferrite core; and ii) Circular coils with ferrite core. The coil dimensions are mentioned in Table 1 and are simulated using Ansys Maxwell and the results are mentioned in the next section.

4. RESULTS AND DISCUSSIONS

As discussed, circular coils with said dimensions are simulated in Ansys Maxwell at a distance of 180 mm (minimum Chassis Clearance of a 4-Wheeler) and Table 2 shows the simulation results of bare coils, coils without ferrites. Frequency after optimization,

$$f_{optimum} = \frac{1}{2\pi \sqrt{L_2 C_2 - \frac{[C_2 (R_L + R_2)]^2}{2}}} = 86.31 \text{ kHz}$$

load resistance value after optimization.

$$R_{L(Opt)} = R_2 \sqrt{1 + \frac{(\omega M)^2}{R_1 R_2}} = 23.413 \Omega$$

Efficiency at which power transfer is happening for circular coil without ferrites is,

$$\eta_{opt} = \frac{k^2 R_L L_1}{k^2 L_1 (R_L + R_2) + R_1 C_2 (R_L + R_2)^2} = 91.62\%$$

Table 2. Simulation results of coils without ferrites - from Ansys simulations

| Sl No | Parameters | Results | Sl No | Parameters | Results |
|-------|------------|----------------|-------|------------|-------------------|
| 1 | L1 | 184.28 μ H | 5 | R1 | 1.023383 Ω |
| 2 | L2 | 184.28 μ H | 6 | R2 | 1.023383 Ω |
| 3 | M | 43.801 μ H | 7 | C1 | 19.02 nF |
| 4 | K | 0.2374 | 8 | C2 | 19.00 nF |

At a frequency of 86.31 kHz, at load resistance of 23.413 Ω , the observed efficiency is 91.62% at an airgap distance of 180 mm. Table 3 gives the observed results at varied coupling coefficient and corresponding efficiency and power transfer level can be observed. The reading highlighted in Table 3 gives the values of various parameters at 180 mm distance.

Table 3. Frequency and load optimization for different coupling coefficient – bare circular coils

| SL.NO | K | F(KHZ) | EFFICIENCY | I1(A) | I2(A) | P1(kW) | P2(kW) | V1(V) | V2(V) |
|-------|--------|--------|------------|-------|-------|--------|--------|--------|--------|
| 1 | 0.15 | 85 | 85.98 | 32.52 | 19.69 | 10.6 | 9.07 | 325.99 | 461.02 |
| 2 | 0.2 | 85 | 90 | 19.12 | 15.48 | 6.219 | 5.613 | 325.11 | 362.53 |
| 3 | 0.2374 | 86.3 | 91.62 | 13.82 | 13.28 | 4.49 | 4.13 | 325.1 | 310.98 |
| 4 | 0.25 | 86.1 | 92.06 | 12.55 | 12.67 | 4.08 | 3.759 | 325.15 | 296.77 |
| 5 | 0.3 | 85.4 | 93.15 | 8.84 | 10.71 | 2.87 | 2.68 | 325.33 | 250.75 |
| 6 | 0.35 | 85 | 93.83 | 6.56 | 9.21 | 2.133 | 1.98 | 325.38 | 215.64 |
| 7 | 0.4 | 85 | 94.28 | 5.018 | 8.12 | 1.63 | 1.54 | 325.36 | 190.13 |
| 8 | 0.45 | 85 | 94.57 | 3.97 | 7.24 | 1.29 | 1.22 | 325.37 | 169.56 |

Figure 7 depicts the circuit diagram analyzed using Ansys Simplorer where, all the circuit parameters including ESR values of Resonant capacitor, DC resistance and AC resistance along with resonant capacitors are considered for the analysis.

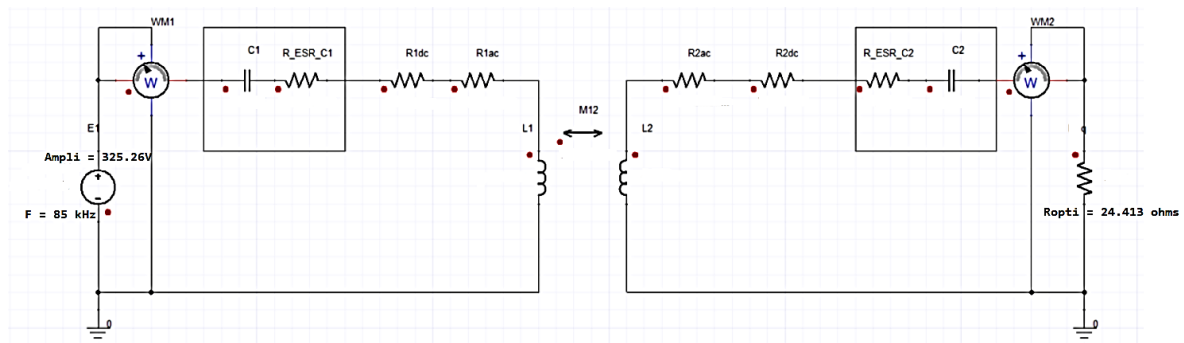


Figure 7. Circuit diagram simulated using Ansys Simplorer

4.1. Circular coils without ferrites

For the circuit shown in Figure 7, AC Sweep analysis and Transient analysis are performed. Many iterations have been done for various distances as mentioned in Table 3. Figure 8 shows results obtained for circular bare coils simulated at 180 mm in Ansys Simplorer.

Figure 8(a) shows the power transferred between primary and secondary coils. Figure 8(b) shows Voltage and Current are in phase with each other portraying resonance is occurring at the primary side. Figure 8(c) clearly shows Resonance occurrence at the secondary side. Figure 8(d) clearly shows the optimum frequency at which maximum efficiency is occurring. Figure 9 depicts the efficiency versus coupling coefficient and frequency for the system based on data from Table 3.

It has been observed that as the coupling coefficient increases, efficacy increases. Also, the Figure 9 shows that the frequency fluctuates with each coupling coefficient. This indicates that the frequency at which the system's efficiency is at its highest is its resonance frequency. Consequently, it is optimal to choose an operating frequency that is near to the system's set resonance frequency. With variations in the load connected to the secondary side, the primary side's total impedance changes. Such variations, i.e., the variance in a vehicle's operating conditions (speed and acceleration.), are prevalent in reality (4Wheeler). The change in load resistance, which occurred in this instance and was therefore proven with regard to equations, was one of the many causes of the impedance variation. The primary side's resonance frequency and output power fluctuate as a result of the impedance's modification. It is significant to notice that at higher values, the resonance frequency separates from the load impedance. Yet, Resonance frequency rises as the impedance falls. Results for circular coils with ferrites were covered in the next section.

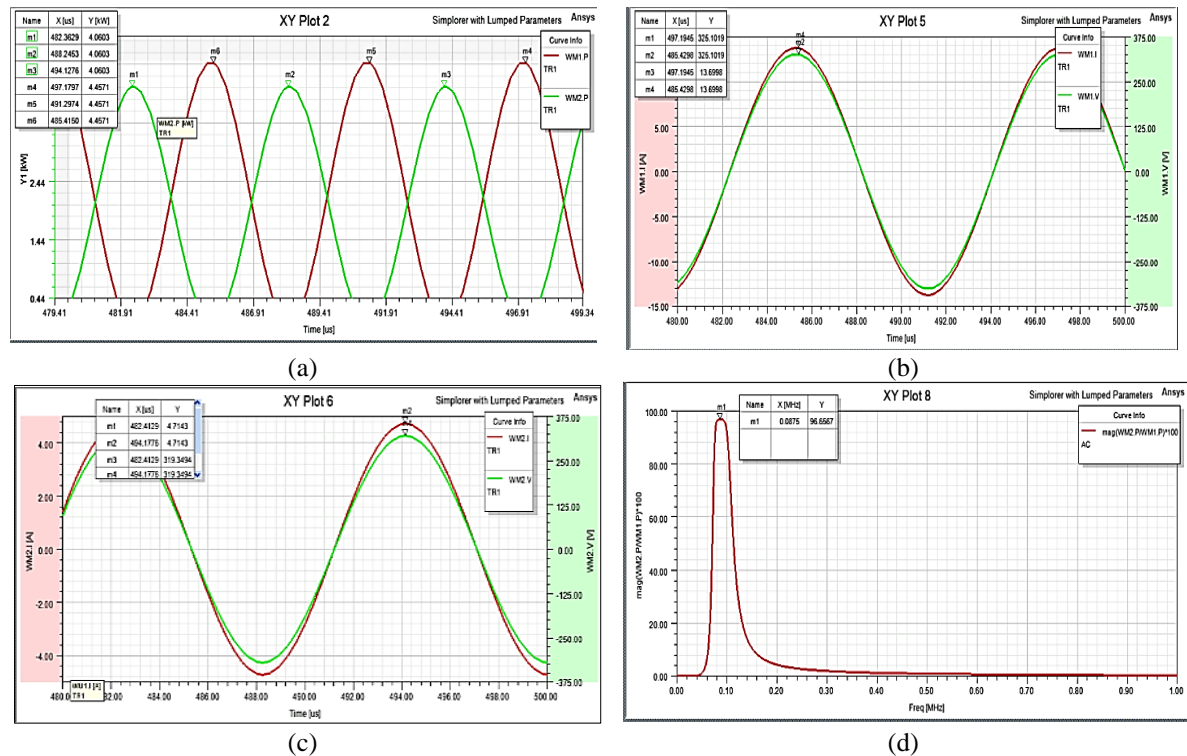


Figure 8. Results obtained of circular bare coils; (a) power transmitted between primary and secondary Winding, (b) transmitter side voltage and current, (c) receiver side voltage and current, and (d) frequency v/s efficiency plot

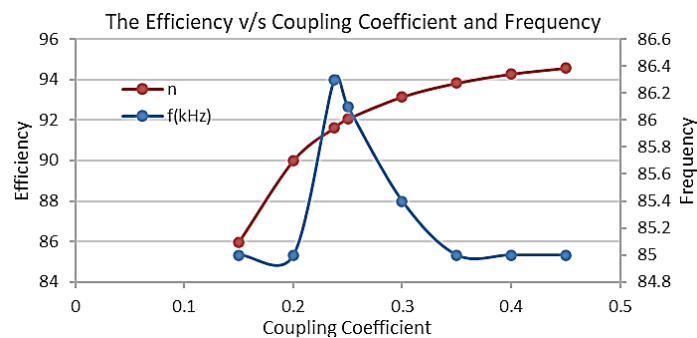


Figure 9. Efficiency, coupling coefficient, and frequency

4.2. Circular coils with ferrites

Consider circular coils of the same dimensions mentioned in Table 1 with ferrite slabs of 2 mm thickness covering the entire area of the coil as shown in Figure 10. Table 4 shows the simulation results of coils with ferrites. Frequency after optimization:

$$f_{\text{optimum}} = \frac{1}{2\pi\sqrt{L_2C_2 - \frac{[C_2(R_L + R_2)]^2}{2}}} = 88.1 \text{ kHz}$$

Load resistance value after optimization:

$$R_{L(\text{Opt})} = R_2 \sqrt{1 + \frac{(\omega M)^2}{R_1 R_2}} = 67.73 \Omega$$

Efficiency at which power transfer is happening for circular coils at 180 mm with ferrites is:

$$\eta_{\text{opt}} = \frac{k^2 R_L L_1}{k^2 L_1 (R_L + R_2) + R_1 C_2 (R_L + R_2)^2} = 96.86\%$$

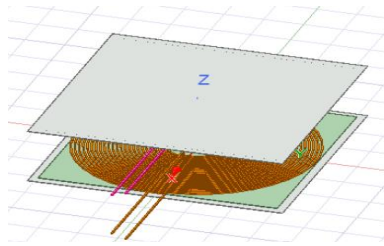


Figure 10. Circular coils with 2 mm ferrite slabs

Table 4. Simulation results of coils with ferrites

| Sl No | Parameters | Results |
|-------|------------|-----------------------|
| 1 | L1 | 347.87 μH |
| 2 | L2 | 347.87 μH |
| 3 | M | 126.813 μH |
| 4 | K | 0.3646 |
| 5 | R1 | 1.0774 Ω |
| 6 | R2 | 1.079 Ω |
| 7 | C1 | 10.08 nF |
| 8 | C2 | 10.07 nF |

At a frequency of 88.1 kHz, at load resistance of 67.73 Ω , the observed efficiency is 96.86% at an airgap distance of 180 mm. There is a significant difference between bare coils and coils with ferrites. Hence, structure of the coil influences the efficiency greatly. Table 5 gives the observed results at varied coupling coefficients, corresponding efficiency, and power transfer levels for the coils with ferrites.

The reading highlighted in Table 5 gives the values of various parameters at 180 mm distance. Figure 11 depicts the circuit diagram analyzed using Ansys Simplorer where, all the circuit parameters including ESR values of resonant capacitor, DC resistance and AC resistance along with resonant capacitors are considered for the analysis with coils having ferrites.

Table 5. Frequency and load optimization for different coupling coefficient – coils with ferrites

| SL.NO | K | F(KHZ) | EFFICIENCY | I1(A) | I2(A) | P1(kW) | P2(kW) | V1(V) | V2(V) |
|-------|--------|--------|------------|-------|-------|--------|--------|--------|--------|
| 1 | 0.15 | 85 | 88.64 | 25.96 | 10.51 | 8.45 | 7.49 | 325.98 | 712.4 |
| 2 | 0.2 | 85 | 92.59 | 15.26 | 8.247 | 4.95 | 4.59 | 325.13 | 558.67 |
| 3 | 0.25 | 85 | 94.53 | 9.97 | 6.739 | 3.24 | 3.0773 | 325.54 | 456.52 |
| 4 | 0.3 | 85 | 95.72 | 7 | 5.68 | 2.2779 | 2.187 | 325.1 | 384.86 |
| 5 | 0.35 | 87.5 | 96.31 | 5.177 | 4.9 | 1.6854 | 1.6305 | 325.09 | 332.18 |
| 6 | 0.3646 | 88.1 | 96.86 | 4.87 | 4.71 | 1.555 | 1.5 | 325.28 | 319.5 |
| 7 | 0.4 | 87.5 | 96.9 | 3.98 | 4.31 | 1.296 | 1.259 | 324.92 | 292.12 |
| 8 | 0.45 | 87.5 | 97.09 | 3.154 | 3.843 | 1.0272 | 1.0018 | 324.88 | 260.34 |

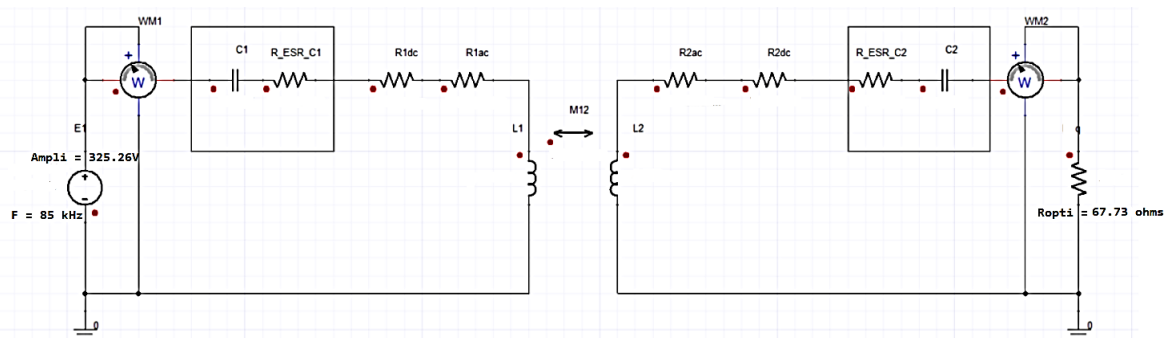


Figure 11. Circuit diagram simulated using ANSYS Simplorer

4.3. Results for coils with ferrites

Figure 12(a) shows the power transferred between primary and secondary for coils with Ferrites. Figure 12(b) shows voltage and current are in phase with each other on the primary side portraying occurrence of resonance. Figure 12(c) shows resonance occurrence at the secondary side. Figure 12(d) depicts the optimum frequency plot at which maximum efficiency of 96.86% is occurring which is way higher than the efficiency of bare coils.

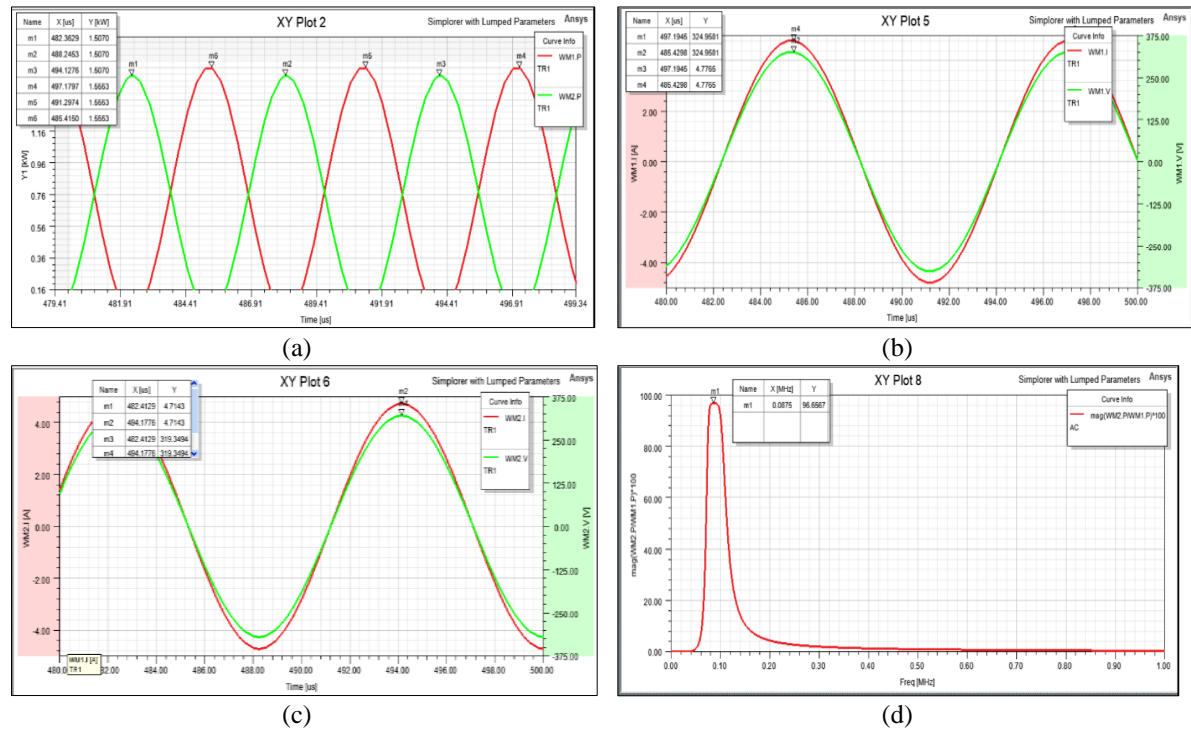


Figure 12. Results obtained of circular coils with ferrites; (a) power transmitted between primary and secondary winding, (b) transmitter side voltage and current, (c) receiver side voltage and current, and (d) frequency v/s efficiency plot.

5. CONCLUSION

In this research, the effectiveness of WPT systems using the resonance approach has been evaluated through simulations. Analytical calculations prove that achieving high efficacy is possible if the conditions of resonance are satisfied. Besides, an optimized load and resonance frequency is required to achieve maximum efficacy. These aspects have been proved with bare coils and coils with ferrites as the core material. The analysis proves coils with ferrites, with load and resonance frequency optimization, demonstrated a superior system performance with higher efficiency of 96.86% which is notably higher than the coils without ferrites. The optimal performance is obtained by loading additional resonance capacitors to both primary and secondary sides of the system. At 180 mm distance, overall performance of the system with higher efficiency is extremely satisfactory.

Hence a coil system considering the design parameters in terms of geometry, coil size, material and frequency is analyzed, and results are tabulated. Among the coils discussed, circular coil is chosen for frequency and load optimization. With a chosen series-series topology and circular coil, the power transfer efficiency achieved is 96.86% using coil with Ferrites in comparison to 91.62% without Ferrites, for the same, in Ansys Simulation. As a future scope a better optimization technique could be used to enhance the PTE for higher lateral distances. The study can be further investigated for different coil geometry and materials. A loss analysis model will help forecast the performance of WPT system with high accuracy.

REFERENCES




- [1] C. C. Mi, G. Buja, S. Y. Choi, and C. T. Rim, "Modern Advances in Wireless Power Transfer Systems for Roadway Powered Electric Vehicles," *IEEE Transactions on Industrial Electronics*, vol. 63, no. 10, pp. 6533–6545, 2016, doi: 10.1109/TIE.2016.2574993.

- [2] B. H. Choi, E. S. Lee, Y. H. Sohn, G. C. Jang, and C. T. Rim, "Six degrees of freedom mobile inductive power transfer by crossed dipole Tx and Rx coils," *IEEE Transactions on Power Electronics*, vol. 31, no. 4, pp. 3252–3272, 2016, doi: 10.1109/TPEL.2015.2449290.
- [3] Y. Zhang, Z. Zhao, and K. Chen, "Load matching analysis of magnetically-coupled resonant wireless power transfer," in *2013 IEEE ECCE Asia Downunder*, Jun. 2013, pp. 788–792. doi: 10.1109/ECCE-Asia.2013.6579192.
- [4] R. Vidya and B. K. Keshaven, "Coil Design for a 3.7kW WPT Electric Vehicle Charger," *13th International Conference on Advances in Computing, Control, and Telecommunication Technologies, ACT 2022*, vol. 8, pp. 1016–1027, 2022.
- [5] Z. H. Ye, Y. Sun, X. Dai, C. Sen Tang, Z. H. Wang, and Y. G. Su, "Energy Efficiency Analysis of U-Coil Wireless Power Transfer System," *IEEE Transactions on Power Electronics*, vol. 31, no. 7, pp. 4809–4817, 2016, doi: 10.1109/TPEL.2015.2483839.
- [6] C. Zhang, D. Lin, and S. Y. Ron Hui, "Ball-Joint Wireless Power Transfer Systems," *IEEE Transactions on Power Electronics*, vol. 33, no. 1, pp. 65–72, 2018, doi: 10.1109/TPEL.2017.2700898.
- [7] R. Bosshard, J. W. Kolar, J. Muhlethaler, I. Stevanovic, B. Wunsch, and F. Canales, "Modeling and η - α - Pareto Optimization of Inductive Power Transfer Coils for Electric Vehicles," *IEEE Journal of Emerging and Selected Topics in Power Electronics*, vol. 3, no. 1, pp. 50–64, Mar. 2015, doi: 10.1109/JESTPE.2014.2311302.
- [8] H. H. Wu, G. A. Covic, J. T. Boys, and A. P. Hu, "A 1kW inductive charging system using AC processing pickups," *Proceedings of the 2011 6th IEEE Conference on Industrial Electronics and Applications, ICIEA 2011*, pp. 1999–2004, 2011, doi: 10.1109/ICIEA.2011.5975920.
- [9] T. Kan, T. D. Nguyen, J. C. White, R. K. Malhan, and C. C. Mi, "A new integration method for an electric vehicle wireless charging system using LCC compensation topology: Analysis and design," *IEEE Transactions on Power Electronics*, vol. 32, no. 2, pp. 1638–1650, 2017, doi: 10.1109/TPEL.2016.2552060.
- [10] L. Zhao, D. J. Thrimawithana, and U. K. Madawala, "Hybrid Bidirectional Wireless EV Charging System Tolerant to Pad Misalignment," *IEEE Transactions on Industrial Electronics*, vol. 64, no. 9, pp. 7079–7086, 2017, doi: 10.1109/TIE.2017.2686301.
- [11] S. Chopra, "Contactless Power Transfer for Electric Vehicle Charging Application," *Science*, no. August, 2011.
- [12] V. Prasanth, "Wireless Power Transfer for E-mobility," no. July, p. 99, 2012.
- [13] L. Chen, S. Liu, Y. C. Zhou, and T. J. Cui, "An optimizable circuit structure for high-efficiency wireless power transfer," *IEEE Transactions on Industrial Electronics*, vol. 60, no. 1, pp. 339–349, 2013, doi: 10.1109/TIE.2011.2179275.
- [14] J. L. Villa, J. Sallan, J. F. Sanz Osorio, and A. Llombart, "High-Misalignment Tolerant Compensation Topology For ICPT Systems," *IEEE Transactions on Industrial Electronics*, vol. 59, no. 2, pp. 945–951, Feb. 2012, doi: 10.1109/TIE.2011.2161055.
- [15] Z. Yuan *et al.*, "High-Order Compensation Topology Integration for High-Tolerant Wireless Power Transfer," *Energies*, vol. 16, no. 2, 2023, doi: 10.3390/en16020638.
- [16] J. Mai, Y. Wang, Y. Yao, and D. Xu, "Analysis and Design of High-Misalignment-Tolerant Compensation Topologies with Constant-Current or Constant-Voltage Output for IPT Systems," *IEEE Transactions on Power Electronics*, vol. 36, no. 3, pp. 2685–2695, 2021, doi: 10.1109/TPEL.2020.3014687.
- [17] M. Rehman, P. Nallagownden, and Z. Baharudin, "Efficiency investigation of SS and SP compensation topologies for wireless power transfer," *International Journal of Power Electronics and Drive Systems*, vol. 10, no. 4, pp. 2157–2164, 2019, doi: 10.11591/ijpeds.v10.i4.pp2157-2164.
- [18] J. A. A. Qahouq and Y. Cao, "Distributed battery system with wireless control and power transfer - A concept introduction," *Conference Proceedings - IEEE Applied Power Electronics Conference and Exposition - APEC*, vol. 2018-March, pp. 344–347, 2018, doi: 10.1109/APEC.2018.8341033.
- [19] S. Ruddell, D. J. Thrimawithana, and U. K. Madawala, "A wireless power transfer system based on a modified full bridge for dynamic EV charging," *Proceedings - 2017 IEEE Southern Power Electronics Conference, SPEC 2017*, vol. 2018-January, pp. 1–5, 2018, doi: 10.1109/SPEC.2017.8333568.
- [20] J. Vazquez, P. Roncero-Sanchez, and A. P. Torres, "Coupling factor of a weak inductive coupling in a 2-kW power transfer system with a 125-mm air gap for electric vehicle chargers," *IEEE International Symposium on Industrial Electronics*, pp. 670–675, 2017, doi: 10.1109/ISIE.2017.8001326.
- [21] B. Klaus, D. Barth, B. Sillmann, and T. Leibfried, "Design and implementation of a transmission system for high-performance contactless electric vehicle charging," *2017 IEEE Transportation and Electrification Conference and Expo, ITEC 2017*, pp. 39–44, 2017, doi: 10.1109/ITEC.2017.7993244.
- [22] S. Wang, J. Chen, Z. Hu, C. Rong, and M. Liu, "Optimisation design for series-series dynamic WPT system maintaining stable transfer power," *IET Power Electronics*, vol. 10, no. 9, pp. 987–995, Jul. 2017, doi: 10.1049/iet-pel.2016.0839.
- [23] S. Li, W. Li, J. Deng, T. D. Nguyen, and C. C. Mi, "A Double-Sided LCC Compensation Network and Its Tuning Method for Wireless Power Transfer," *IEEE Transactions on Vehicular Technology*, vol. 64, no. 6, pp. 2261–2273, 2015, doi: 10.1109/TVT.2014.2347006.
- [24] S. L. Ho, J. Wang, W. N. Fu, and M. Sun, "A comparative study between novel witricty and traditional inductive magnetic coupling in wireless charging," *IEEE Transactions on Magnetics*, vol. 47, no. 5, pp. 1522–1525, 2011, doi: 10.1109/TMAG.2010.2091495.
- [25] K. W. Klontz, D. M. Divan, D. W. Novotny, and R. D. Lorenz, "Contactless power delivery system for mining applications," *1991 IEEE Industry Application Society Annual Meeting*, pp. 1263–1269, 1991, doi: 10.1109/ias.1991.178024.
- [26] J. Sallán, J. L. Villa, A. Llombart, and J. F. Sanz, "Optimal design of ICPT systems applied to electric vehicle battery charge," *IEEE Transactions on Industrial Electronics*, vol. 56, no. 6, pp. 2140–2149, 2009, doi: 10.1109/TIE.2009.2015359.
- [27] X. Liu, W. M. Ng, C. K. Lee, and S. Y. Hui, "Optimal operation of contactless transformers with resonance in secondary circuits," *Conference Proceedings - IEEE Applied Power Electronics Conference and Exposition - APEC*, pp. 645–650, 2008, doi: 10.1109/APEC.2008.4522790.
- [28] W. Chen, W. Lu, and X. Wang, "Circuit modeling and efficiency analysis for wireless power transfer system with shielding," *International Journal of Circuit Theory and Applications*, vol. 47, no. 2, pp. 294–303, 2019, doi: 10.1002/cta.2589.
- [29] M. Heidarian and S. J. Burgess, "A Design Technique for Optimizing Resonant Coils and the Energy Transfer of Inductive Links," *IEEE Transactions on Microwave Theory and Techniques*, vol. 69, no. 1, pp. 399–408, 2021, doi: 10.1109/TMTT.2020.3028969.
- [30] H. Lee and B. Lee, "Investigation of MIMO Wireless Power Transfer Efficiency in Optimization Techniques," *2020 IEEE International Symposium on Antennas and Propagation and North American Radio Science Meeting, IEEECONF 2020 - Proceedings*, pp. 1417–1418, 2020, doi: 10.1109/IEEECONF35879.2020.9330339.
- [31] A. O. El Meligy, E. A. Elghanam, M. S. Hassan, and A. H. Osman, "Deployment Optimization of Dynamic Wireless Chargers for




- Electric Vehicles,” 2022 *IEEE Transportation Electrification Conference and Expo, ITEC 2022*, pp. 290–294, 2022, doi: 10.1109/ITEC53557.2022.9813969.
- [32] T. H. Abdelhamid, A. Elzawawi, and M. A. Elreazek, “Wireless Power Transfer Analysis and Power Efficiency Enhancement via Adaptive Impedance Matching Network,” *ICPEA 2021 - 2021 IEEE International Conference in Power Engineering Application*, pp. 91–96, 2021, doi: 10.1109/ICPEA51500.2021.9417839.
- [33] B. M. Patil and S. Y. Gadgune, “Review of wireless power transfer for EV with advancement in designs,” *2021 5th International Conference on Electrical, Electronics, Communication, Computer Technologies and Optimization Techniques, ICECCOT 2021 - Proceedings*, pp. 44–48, 2021, doi: 10.1109/ICECCOT52851.2021.9707979.
- [34] T. Muni Prakash *et al.*, “A Review on Optimization Techniques of Charging the Battery in EV,” *Proceedings of the 2nd International Conference on Artificial Intelligence and Smart Energy, ICAIS 2022*, pp. 799–804, 2022, doi: 10.1109/ICAIS53314.2022.9743126.
- [35] T. Wang, Y. Wu, B. Li, Q. Yu, L. Xu, and S. Guan, “Design of Electric Vehicle’s Wireless Power Transfer System Based on Deep Learning Combined With Multi-Objective Optimization,” *IEEE Transactions on Components, Packaging and Manufacturing Technology*, vol. 12, no. 12, pp. 1983–1994, 2022, doi: 10.1109/TCPMT.2022.3222841.
- [36] B. Ouacha, H. Bouyghf, M. Nahid, S. Abenna, and L. Zougagh, “A comparative analysis of metaheuristic techniques for improving PTE and PDL of a wireless power transfer system,” *2022 IEEE 3rd International Conference on Electronics, Control, Optimization and Computer Science, ICECOCS 2022*, 2022, doi: 10.1109/ICECOCS55148.2022.9983105.
- [37] M. Iordache, M. Stanculescu, D. Niculae, L. Bobaru, S. Deleanu, and O. Drosu, “Wireless Power Transfer Systems Optimization,” in *2022 International Conference and Exposition on Electrical And Power Engineering (EPE)*, Oct. 2022, pp. 130–134. doi: 10.1109/EPE56121.2022.9959759.

BIOGRAPHIES OF AUTHORS



Raja Vidya    is an Assistant Professor in the Department of Electrical and Electronics Engineering, RV College of Engineering, Bengaluru, India with 14 Yrs. of Experience. Received B.Engg. degree in Electrical and Electronics Engineering from Kuvempu University, Karnataka 2001, M.Tech. degree in VLSI & Embedded systems from VTU 2010, Karnataka. At present pursuing Ph.D degree from VTU, Belagavi, Karnataka, India. Research areas include but not limited to Electric Vehicles, Wireless Power transfer technologies, Battery Management systems, Battery Technologies, Charging Infrastructure and Renewable Integration. She can be contacted by email: rajavidya@rvce.edu.in.



Belur K. Keshavan    is Professor and Head in the Department of Electrical & Electronic Engineering, PES University, Bangalore, India since 2007 and he has been Chairperson, Department of Electrical and Electronics Engineering and Dean -Faculty of Engineering & Technology, PES University. He received the B.Engg. degree in Electrical Engineering from M.C.E.Hassan 1980, M.Engg. degree from P.S.G. College of Technology, Coimbatore 1989 and Ph.D. degree from IIT Bombay 1998. He is in various committees like Member B.O.E., V.T.U for 3 years, Member - Academic council-PESU, Chairman B.O.E., V.T.U etc. His research areas include but not limited to Power System Reliability, Distribution System Management, FACTS, Energy auditing, Electrical Machines, smart grid, renewable energy sources, Battery Management system. He has done many research Publications in Reputed Journals and conferences in the areas of Testing of Electrical Equipment like Transformers, Motors, Rectifiers, Energy Auditing, reliability evaluation of power systems, Smart grid and Distribution system management. He received "Centre of Excellence in High Voltage & Power System" - Vision Group on Science and Technology, Department of Science and Technology, Govt. of Karnataka. He can be contacted by email: keshavanbk@pes.edu.